

Accepted Manuscript

Novel synthetic approach, spectroscopic characterization and theoretical studies on global and local reactive properties of a bibenzimidazolyl derivative

Kollur Shiva Prasad, Nagaraj Nayak, Renjith Raveendran Pillai, Stevan Armačić, Sanja J. Armačić



PII: S0022-2860(17)30854-2

DOI: [10.1016/j.molstruc.2017.06.073](https://doi.org/10.1016/j.molstruc.2017.06.073)

Reference: MOLSTR 23959

To appear in: *Journal of Molecular Structure*

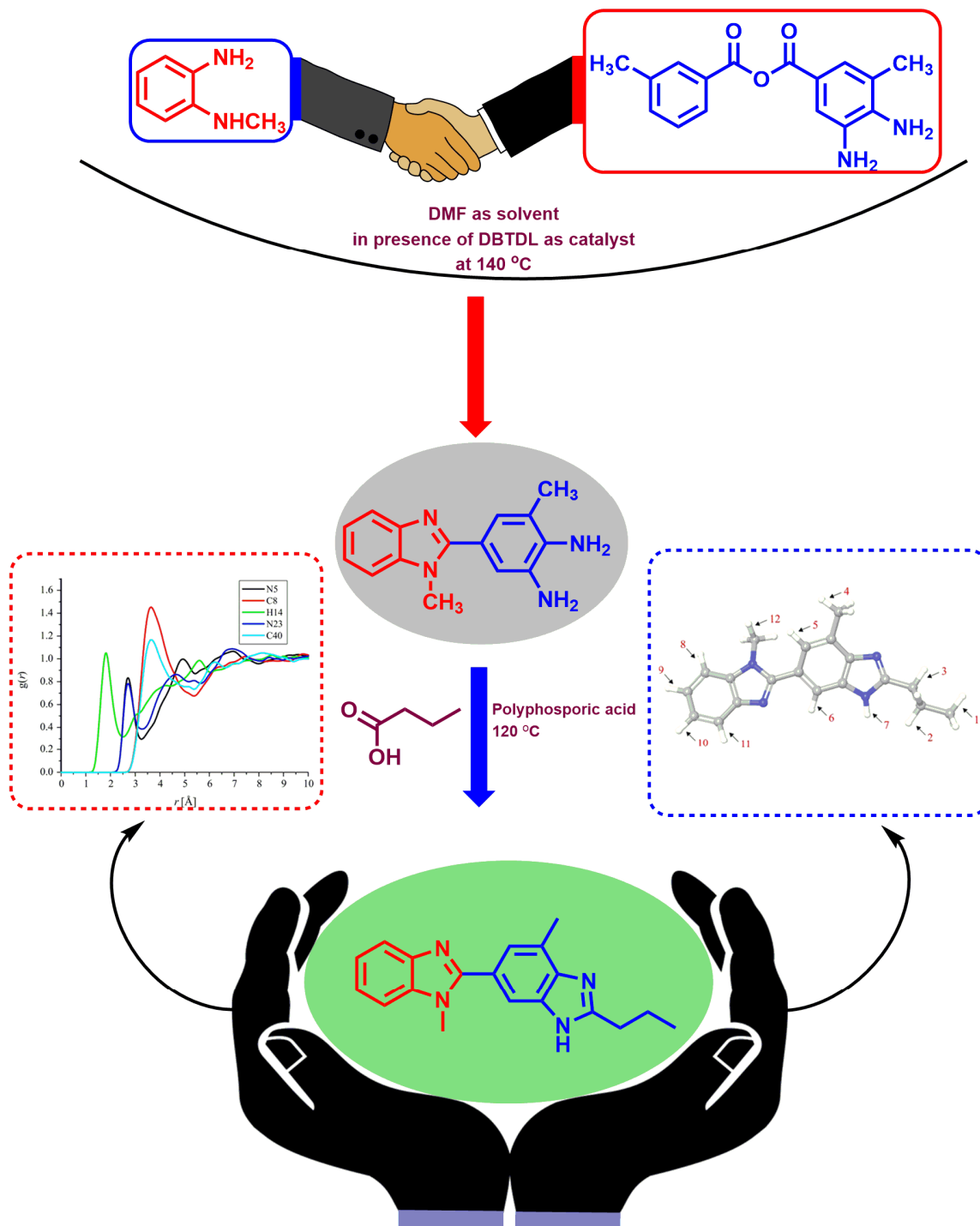
Received Date: 7 April 2017

Revised Date: 16 June 2017

Accepted Date: 16 June 2017

Please cite this article as: K.S. Prasad, N. Nayak, R.R. Pillai, S. Armačić, S.J. Armačić, Novel synthetic approach, spectroscopic characterization and theoretical studies on global and local reactive properties of a bibenzimidazolyl derivative, *Journal of Molecular Structure* (2017), doi: 10.1016/j.molstruc.2017.06.073.

This is a PDF file of an unedited manuscript that has been accepted for publication. As a service to our customers we are providing this early version of the manuscript. The manuscript will undergo copyediting, typesetting, and review of the resulting proof before it is published in its final form. Please note that during the production process errors may be discovered which could affect the content, and all legal disclaimers that apply to the journal pertain.

Graphical Abstract (pictogram)

Novel synthetic approach, spectroscopic characterization and theoretical studies on global and local reactive properties of a bibenzimidazolyl derivative

Kollur Shiva Prasad^{a*}, Nagaraj Nayak^a, Renjith Raveendran Pillai^b, Stevan Armaković^c, Sanja J. Armaković^d

^a *Laboratory of Synthetic and Materials Chemistry, Manipal Centre for Natural Sciences, Manipal University, Karnataka – 576104, India.*

^b *Department of Physics, TKM College of Arts and Science, Karicode, Kollam, Kerala - 69100, India.*

^c *University of Novi Sad, Faculty of Sciences, Department of Physics, Trg D. Obradovića 4, 21000 Novi Sad, Serbia.*

^d *University of Novi Sad, Faculty of Sciences, Department of Chemistry, Biochemistry and Environmental Protection, Trg D. Obradovića 3, 21000 Novi Sad, Serbia.*

*Corresponding author email: shivachemist@gmail.com (K. Shiva Prasad)

Abstract

Benzimidazole derivatives are of interest because they can exhibit multi-drug like properties and thus finds wide applications in biomedicine. Present work describes a novel route for the synthesis of a benzimidazole derivative, 1,7'-Dimethyl-2'-propyl-1H,3'H-[2,5']bibenzoimidazolyl (**R4**) by using dibutyltin dilaurate (DBTDL) as catalyst. The catalyst, DBTDL is commercial and environmentally benign. The molecular structure of **R4** was confirmed by FT-IR, ¹H, ¹³C NMR, and mass spectrometry techniques. The detailed reactivity study of **R4** encompasses spectroscopic characterization and computational investigations of global and local reactive properties based on the density functional theory (DFT) and time dependent density functional theory (TD-DFT) calculations, and molecular dynamics (MD) and molecular docking (MDoc) simulations. Global reactive properties of the title compound have been investigated by the

analysis of frontier molecular orbitals. Local reactive properties have been investigated by the analysis of quantum-molecular descriptors such as molecular electrostatic potential (MEP), average local ionization energy (ALIE) surfaces, and Fukui functions. Bond dissociation energies (BDE) have been calculated in order to determine molecule sites that could be sensitive towards the autoxidation mechanism, while the radial distribution functions have been calculated in order to determine atoms with the significant interactions with water molecules.

Keywords: Benzimidazole, Dibutyltin dilaurate, Spectroscopy, DFT studies.

1. Introduction

The design and synthesis of benzimidazole derivatives have attracted much attention in last decade or so due to their wide applications and their therapeutic importance [1-3]. There are several reports on synthesis of benzimidazole such as the reductive cyclization of o-nitroanilines with aldehydes [4], cyclization of o-nitroaniline derivatives with aryl isothiocyanates [5], and Baker's yeast reduction of 2,4-dinitroacyl anilines [6]. Primary role of pharmaceutical compounds is to help, however this class of materials also has significant negative ecological impact to the environment [7-11]. For this reason scientific community is highly devoted to understanding fundamental reactive properties of pharmaceutical molecules. Most recently, we reported reactivity and photophysical properties of Schiff bases and their Co(II) and Mn(II) complexes based on ALIE and TDDFT studies [12].

Herein, we report the synthesis of benzimidazole derivative, 1,7'-Dimethyl-2'-propyl-1H,3'H-[2,5']bibenzoimidazolyl (**R4**) by novel approach in presence DBTDL as catalyst and demonstrate its BDE. Since, oxidation is frequently employed tool for degradation of drugs [13], in this work

we have calculated the BDE for hydrogen atoms (H-BDE) in order to evaluate the sensitivity of target molecule towards autoxidation mechanism [14-17]. Beside H-BDE and autoxidation mechanism we were also focused to determine which atoms of **R4** molecule have the most pronounced interactions with water molecules, since hydrolysis mechanism is also very important for the degradation of drugs.

2. Experimental

2.1. Materials and methods

3-methylbenzene-1,2-diamine was procured from Thermo Fisher Scientific (USA), 3-Methyl-5-(1-methyl-1H-benzimidazol-2-yl)-benzene-1,2-diamine and dibutyltin dilaurate were obtained from Sigma Aldrich chemicals (USA). The solvents and other chemical reagents were purchased from Merck chemicals (India) and were dried and purified by standard methods prior to use. FT-IR spectral measurements were made on Perkin-Elmer spectrometer version 10.03.09 (KBr pellet technique). ^1H and ^{13}C NMR were obtained using a 500 MHz Bruker Avance DPX spectrometer with TMS as internal standard. Mass spectra (HR-ESI) was recorded on a Thermo Scientific-Q-Exactive Hybrid Quadrupole-Orbitrap mass spectrometer by electrospray ionization technique. The completion of reaction was monitored by thin layer chromatography (TLC) performed on precoated silica-gel plates (Merck, India) and spots were visualized by UV irradiation. The purification of compound was done by flash chromatography using Biotage instrument.

2.2. Computational Details

In this work computational studies have been performed by employing the Schrödinger Materials Science Suite 2017-1 [18]. DFT calculations have been performed with Jaguar 9.5 program [19], while MD simulations have been performed with Desmond program [20-23]. A hybrid, non-local exchange and correlation functional of Becke-Lee, Parr i Yang (B3LYP) [24] has been used with

the 6-311++G(d,p), 6-31+G(d,p) and 6-311G(d,p) for the calculations of ALIE, Fukui functions and BDEs, respectively. For calculations based on time dependent density functional theory (TD-DFT) approach we have used CAM-B3LYP [25] long range corrected functional with 6-31+G(d,p) basis sets in full linear response.

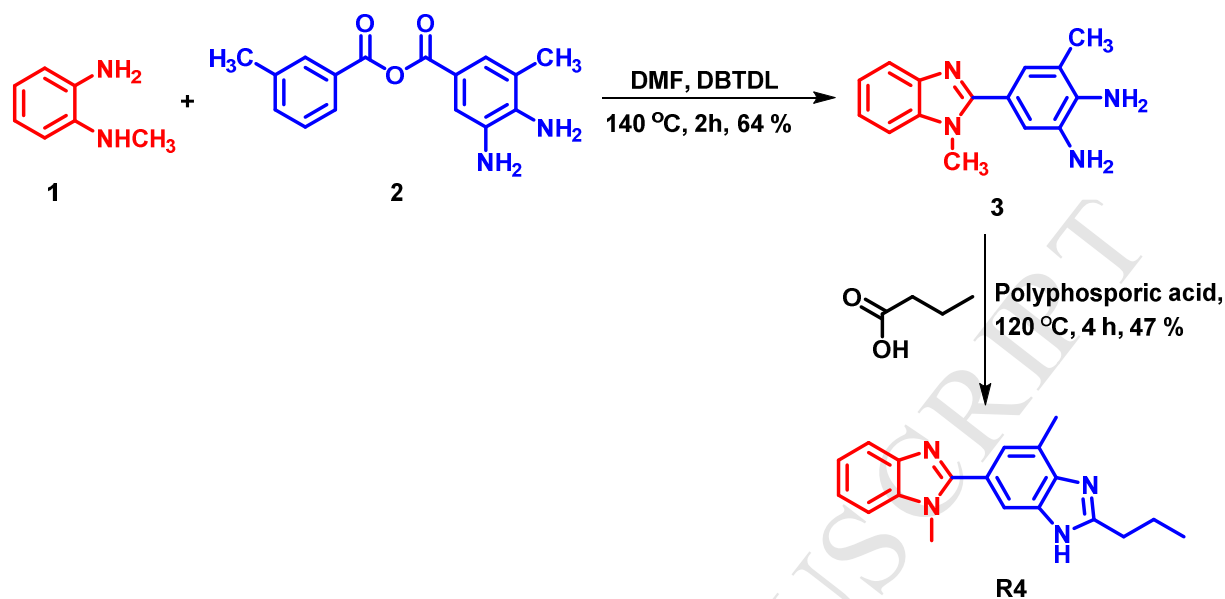
The lowest energy conformation has been obtained by detailed conformational search employing MacroModel program, also as incorporated in the Schrödinger Materials Science Suite 2017-1. Conformational search yielded 27 structures of which the lowest energy one was chosen for further calculations. Conformational search in MacroModel has been performed with OPLS3 force field and without constraints and employing the mixed torsional and low mode sampling. Cut off during conformational search was set to normal, while charges were taken from the force field. Maximum number of steps during conformational search was set to 1000, with 100 steps per rotatable bond. Energy window for saving structures was 5.02 kcal/mol, while elimination of redundant conformers was done by maximum atom deviation with cutoff of 0.5 Å. Probability of a torsion rotation/molecule translation was 0.5, minimum distance for low mode move was 3.0, while maximal was 6.0.

MD simulations have been performed with OPLS 3 force field [20, 26-28], with simulation time set to 10 ns, temperature to 300 K, pressure to 1.0325 bar and cut off radius to 12 Å. System was of isothermal–isobaric (NPT) ensemble class. Simple point charge (SPC) solvent model [29] was used as well. In order to model the system for MD simulations one **R4** molecule has been placed in cubic box along with ~3000 water molecules. Intramolecular non-covalent interactions were determined by electron density analysis employing the method developed by Johnson *et al.* [30, 31] Maestro GUI [32] was used for the preparation of input files and analysis of results when Schrödinger Materials Science Suite 2017-1 was employed.

2.3. Synthesis of 1,7'-Dimethyl-2'-propyl-1H,3'H-[2,5']bibenzoimidazolyl (**R4**)

The synthesis of target compound, **R4** was instigated with the conversion of commercially available 3-methylbenzene-1,2-diamine (**1**) to 3-Methyl-5-(1-methyl-1H-benzoimidazol-2-yl)-benzene-1,2-diamine (**3**) using previously reported method with minor modifications [33]. As shown in Scheme 1, compound **3** was obtained by acylation/dehydration condensation sequence of **1** with m-tolyl derivative **2** in the presence of dibutyltin dilaurate (DBTDL) as catalyst in DMF at 140 °C for 2 h. Treatment of the resulting benzoimidazole-1,2-diamine derivative **3** with butyric acid and polyphosphoric acid at 120 °C for 4 h afforded target compound **R4** in moderate yield.

Yield: 47%. FT-IR (KBr, cm^{-1}): 1385-1328 cm^{-1} (Aromatic C-N stretch), 3390 cm^{-1} (heterocyclic NH stretch), 1515-1461 cm^{-1} (Aromatic C-H stretch) and 2964-2871 cm^{-1} (Aromatic propyl stretch). ^1H NMR (500 MHz, CDCl_3 , ppm): $\delta = 7.30-7.77$ (6H, m, $J = 7.5$ Hz, Ar-H), $\delta = 3.86$ (3H, s, N- CH_3), $\delta = 2.72-2.69$ (2H, t, $J = 7$ Hz, CH_2), $\delta = 2.48$ (3H, s, Ar- CH_3), $\delta = 1.73-1.66$ (2H, sextet, $J = 7$ Hz, CH_2), $\delta = 0.81-0.78$ (3H, t, $J = 7.5$ Hz, CH_3). ^{13}C NMR (125 MHz, CDCl_3 , ppm): $\delta = 157.30, 155.34, 142.28, 136.41, 122.69, 122.58, 118.78, 109.87, 31.80, 31.15, 21.77, 17.12, 13.76$. MS (ESI): $[\text{M}^+] = 304.17$; Expt. Found: 305.17 $[\text{M}^+ + 1]$.



Scheme 1: Synthetic pathway of bibenzoimidazolyl derivative, **R4** from *N*-methyl-benzene-1,2-diamine.

3. Results and discussion

The structure elucidation of synthesized compound was done using FT-IR, ^1H , ^{13}C NMR, and mass spectral techniques. The yield and spectral characterization for **R4** molecule is depicted in synthesis section. The FT-IR spectrum showing characteristic band at 3390 cm^{-1} , indicating the presence of $-\text{NH}$ stretching; and sharp bands, observed between $1385\text{--}1328\text{ cm}^{-1}$ indicates the presence of C-N stretch. The presence of aromatic propyl stretch was confirmed by observing sharp bands in the range $2964\text{--}2871\text{ cm}^{-1}$. The further confirmation of molecular structure was done by ^1H and ^{13}C NMR spectral analysis. A singlet peak observed at 3.86 ppm was attributed to methyl protons of N- CH_3 group and another singlet peak observed at 2.48 ppm was ascribed for protons of methyl group attached directly to aromatic ring. A triplet peak between 0.87-0.78 ppm was assigned to free methyl protons of aromatic propyl moiety. Similarly, a sextet and a triplet observed between 1.78-1.66 and 2.72-2.69 ppm were due to two methylene group protons under different environment in aromatic propyl group, respectively. The aromatic protons were

seen around 7.29-7.77 ppm region. In support to this, ^{13}C NMR spectral data also revealed the presence of imidazole rings at 157.30 and 155.34 ppm. Further appearance of the molecular ion peak at 305.17 ($M + 1$) confirmed the structure of **R4**.

3.1. ALIE surface, Fukui functions and non-covalent interactions

MEP surfaces are usually employed for the determination of molecule sites that are prone to electrophilic and nucleophilic attacks. However, for these purposes it is more efficient to use ALIE surfaces, as they directly indicate molecule sites where electrons are least tightly bonded and therefore they are easily removed from the molecule [34-37]. The lowest values on the ALIE surfaces indicate areas where molecules are the most sensitive towards electrophilic. In this regard, ALIE surfaces are considered as one of the most useful quantum-molecular descriptors reflecting the local reactivity properties of molecules [38-41]. The most representative ALIE surface of the title molecule (**R4**) is presented in Figure 1, where red color denotes the lowest ALIE values, while purple color denotes the highest ALIE values.

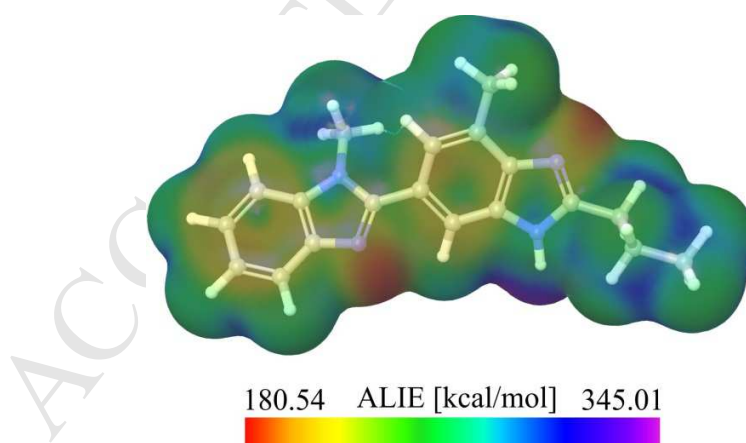


Figure 1. ALIE surface of **R4** molecule.

The target molecule **R4** has a specific ALIE surface indicating two distinct molecule sites where ALIE values are taking the lowest values. These two molecule sites are nitrogen atoms of five membered rings (N5 and N23), characterized by the ALIE values of ~151 kcal/mol. One five membered ring is also important from the aspect of the highest ALIE value. Namely, the highest ALIE values (~345 kcal/mol) is located in the vicinity of hydrogen atom H14. In the case of **R4** molecule only one intramolecular non-covalent interaction has been determined. It is located between hydrogen atoms H34 and H42, with the strength equal to 0.010 electron/bohr³.

The concept of Fukui functions allowed us to further identify important reactive molecule sites after the addition or removal of charge. Namely, Fukui functions track the changes in electron density after the addition or removal of charge, according to the following equations

$$f^+ = \frac{(\rho^{N+\delta}(r) - \rho^N(r))}{\delta}, \quad (2)$$

$$f^- = \frac{(\rho^{N-\delta}(r) - \rho^N(r))}{\delta}. \quad (3)$$

where N stands for the number of electrons in reference state of the molecule, while δ stands for the fraction of electron which default value is set to be 0.01 [42]. Fukui functions values can be mapped to the electron density surface in order to easily detect reactive sites of the molecule. Representative electron density surfaces with mapped values of Fukui functions for the **R4** molecule have been presented in Figure 2.

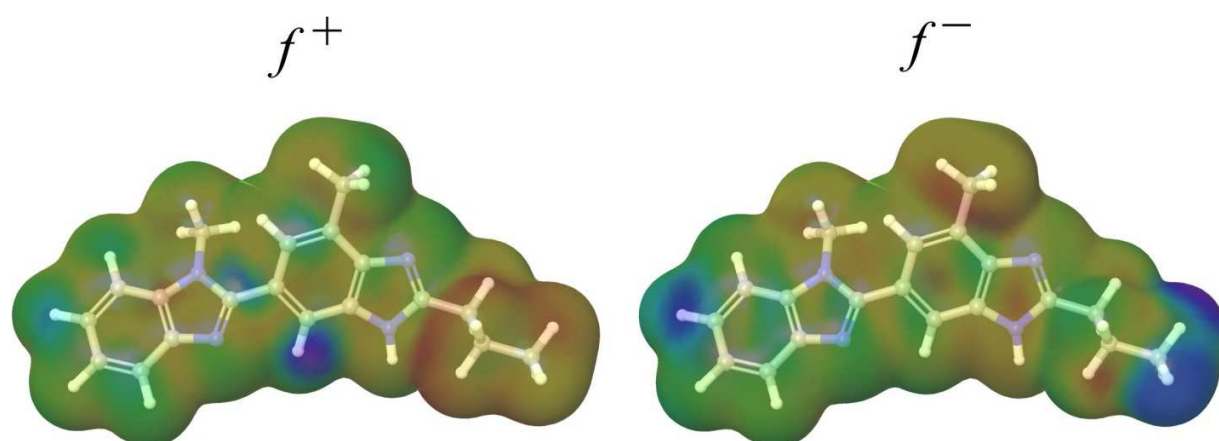


Figure 2. Fukui functions of **R4** molecule.

Positive value of Fukui f^+ function is purple colour and it can be seen in Figure 2 that in the case of **R4** molecule it is located in the vicinity of hydrogen atom H35, designating the molecule site where electron density increases after the addition of charge to the **R4** molecule. On the other side negative color in the case of Fukui f^- function is located in the near vicinity of methyl group attached to the benzene ring and in the vicinity of hydrogen atom H28 of the alkyl chain, marking these locations as the ones where electron density decreases after the removal of charge.

3.2. Reactive and degradation properties based on autoxidation and hydrolysis

Taking into an account of the importance of oxidative degradation of pharmaceutical molecules further, we investigated how sensitive **R4** molecule is towards the mechanism of autoxidation [43-46]. Sensitivity of some organic molecules towards autoxidation mechanism can be evaluated by performing the calculation of H-BDEs [13, 47, 48]. In the same time, sensitivity of some organic molecule to the influence of water can be evaluated by RDFs.

H-BDE values in the interval between 70 to 85 kcal/mol [49, 50] indicate sensitivity towards autoxidation mechanism, while values between 85 and 90 kcal/mol could be interesting for autoxidation mechanism but also should be taken with caution [50]. One could mistakenly

conclude that H-BDE should be as low as possible, but that isn't the case because values lower than 70 kcal/mol are not appropriate for the autoxidation mechanism [14, 50, 51]. H-BDE values for the **R4** molecule have been calculated and the results are presented in Figure 3.

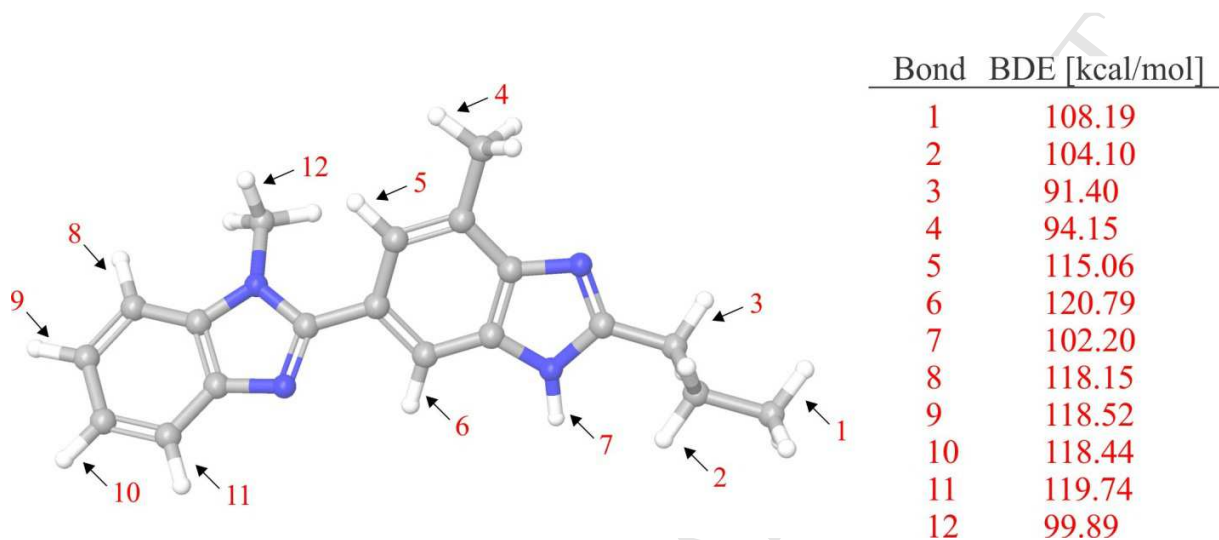


Figure 3. H-BDEs in the case of **R4** molecule.

In Figure 3 it can be seen that there aren't H-BDE values in the preferred range between 70 and 85 kcal/mol. Although there is one H-BDE value, located at the beginning of alkyl chain, close to the upper border level of 90 kcal/mol, its value is still above the desired threshold. All other H-BDE values are substantially higher than 90 kcal/mol, thus it can be concluded that the **R4** molecule is stable towards the autoxidation mechanism and that it could be highly stable in the open air, which prolongs its durability but also hardens its degradation under natural conditions.

To detect the atoms of **R4** molecule that have pronounced interactions with water molecules we further mentioned the results concerning the RDFs in Figure 4. RDF denotes probability of finding a particle in the distance r with respect to another particle [52]. RDFs represent a precious MD tool when it comes to the investigation of structuring around atoms or molecules of interest [53-61]. In this work we have used the concept of RDFs we were able to

determine which atom of **R4** molecule have pronounced interactions with water molecules. High and sharp peaks of $g(r)$ curves indicate high probability of finding a water molecule (with respect to oxygen atoms) at certain distance of the observed atom of investigated molecule. The more the highest $g(r)$ values are located at the shorter distances, the more pronounced are the interactions.

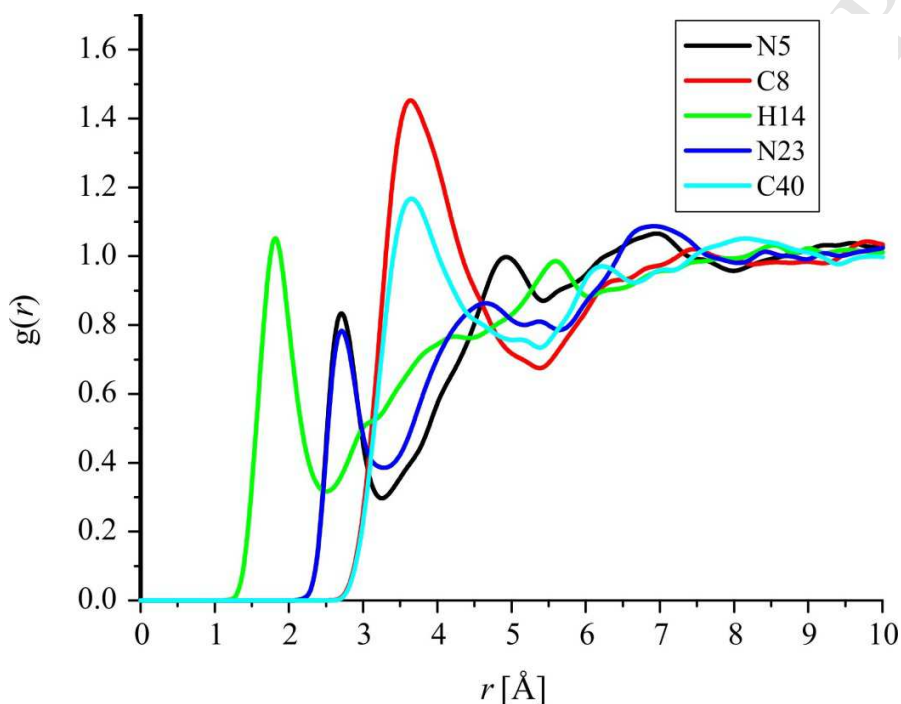


Figure 4. Significant RDFs of atoms of **R4** molecule.

MD system was prepared by corresponding system setup module of Maestro, while the number of water molecules was manipulated by the dimensions of the simulation box. Radial distribution functions have been calculated by the corresponding module of Maestro, with respect to the distance between observed atom of **R4** molecule and the oxygen atom of water molecule. Results presented in Figure 4 show that **R4** molecule has five atoms with relatively important interactions with water molecules. These five atoms are two carbon atoms (C8 and C40), two nitrogen atoms (N5 and N23) and one hydrogen atom (H14). Of all these atoms the most important RDF has been noticed in the case of hydrogen atom H14. Since its maximal $g(r)$ value

is located at the distance lower than 2 Å, it can be stated that **R4** has relatively significant interactions with water molecules. Two aforementioned nitrogen atoms have their maximal $g(r)$ values located at distances around 2.7 Å and these two RDFs are almost identical. Locations of two nitrogen atoms indicate the importance of five membered rings, when it comes to the interactions with water molecules. The difference between the two five membered rings is the fact that one has methyl group while other has only hydrogen atom. That makes significant difference between them because hydrogen atom H14 has the most important RDFs and interactions with water molecules, thus it can be stated that corresponding five membered ring is much more reactive. The importance of hydrogen atom H14 is also reflected by the ALIE surface in Figure 1, according to which precisely this atom is characterized by the highest ALIE values. Although two carbon atoms have the highest maximal $g(r)$ values, their maximums are located at distance higher than 3.5 Å. Both of these carbon atoms are belonging to methyl groups.

3.3. TD-DFT study of **R4** molecule

In the present work we have performed TD-DFT calculations in order to obtain computational UV spectrum of the **R4** molecule, while analysis of natural transition orbitals [62] (NTO) allowed us to identify the most important excitations and molecule parts mainly responsible for light absorption. Firstly, we will provide comparison of experimentally measured and theoretically obtained UV spectra in order to validate the employed level of theory. Figure 5 contains experimentally and computationally obtained UV spectra of **R4** molecule.

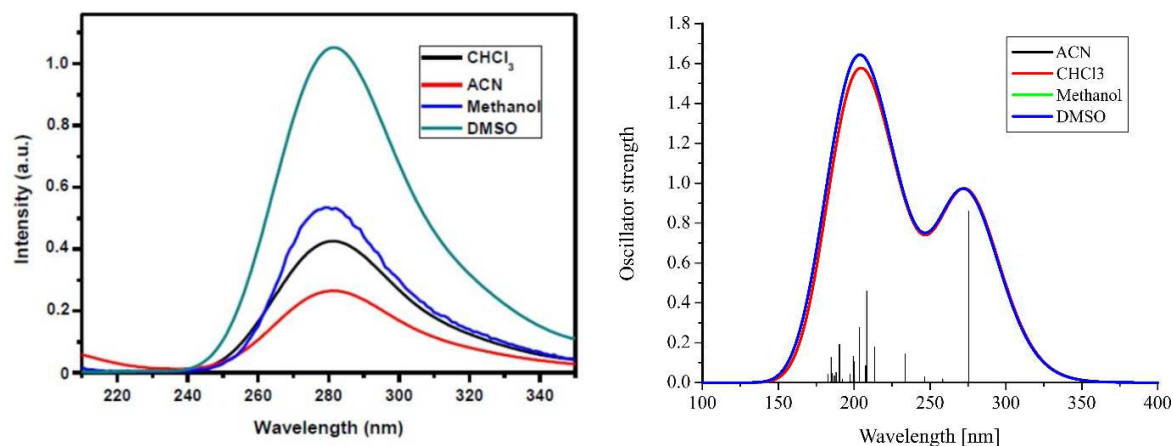


Figure 5. Experimental (right) and theoretical (left) UV spectra of **R4** in different solvents.

Both experimentally and computationally obtained UV spectra show the existence of two main absorption peaks. Comparison of results indicates very good agreement when it comes to the position of absorption peaks, especially the one located at around 280 nm. Namely, experimentally measured UV spectrum indicates the existence of absorption peak at 280 nm, while theoretically obtained absorption peak is located at 276 nm.

The most important electronic transitions have been further analyzed in detail. The molecule under investigation was relatively large so TD-DFT calculations provided large list of orbital transitions, which hardened the identification of the dominant components. For better qualitative description of the most important electronic excitations, the concept of natural transition orbitals (NTO) [62] has been adopted and the calculations had been done with Jaguar program. Contrary to ordinary orbitals, NTOs consists of one (sometimes two or more) pair of orbitals with NTO transition occurring from excited particle (occupied) to the empty hole (unoccupied) orbital [62]. In Figure 6 we have provided frontier molecular orbitals (HOMO and LUMO) and hole-particle orbitals of the two most important excitations (important according to the values of oscillator

strengths). Table 1 contains information on excitation energies, wavelength and oscillator strengths of the first twenty excitations.

Table 1. Information about the first 20 excitations of **R4** molecule.

| Excitation # | Excitation energy [eV] | Wavelength [nm] | Oscillator strength |
|--------------|------------------------|-----------------|---------------------|
| 1 | 4.50 | 275.60 | 0.8548 |
| 2 | 4.80 | 258.37 | 0.0145 |
| 3 | 5.03 | 246.47 | 0.0250 |
| 4 | 5.31 | 233.70 | 0.1411 |
| 5 | 5.80 | 213.60 | 0.1765 |
| 6 | 5.95 | 208.31 | 0.4530 |
| 7 | 5.97 | 207.70 | 0.0793 |
| 8 | 6.09 | 203.57 | 0.2728 |
| 9 | 6.19 | 200.36 | 0.0361 |
| 10 | 6.19 | 200.17 | 0.1005 |
| 11 | 6.22 | 199.41 | 0.1252 |
| 12 | 6.28 | 197.47 | 0.0035 |
| 13 | 6.29 | 197.23 | 0.0387 |
| 14 | 6.45 | 192.28 | 0.0136 |
| 15 | 6.51 | 190.37 | 0.1870 |
| 16 | 6.59 | 188.23 | 0.0466 |
| 17 | 6.63 | 186.88 | 0.0302 |
| 18 | 6.68 | 185.71 | 0.0420 |
| 19 | 6.70 | 184.94 | 0.1211 |
| 20 | 6.78 | 182.92 | 0.0391 |

Results presented in Table 1 indicate that the lowest energy excitation, with excitation energy of 4.50 eV, is mainly responsible for the absorption peak of **R4** molecule at 276 nm. The oscillator strength for this excitation is the highest and it takes the value of 0.8548. Running-up excitation mainly contributing to the absorption peak at around 200 nm is the sixth excitation with the oscillator strength value of 0.4530. NTOs related to these two excitations have been presented in Figure 6, together with HOMO and LUMO.

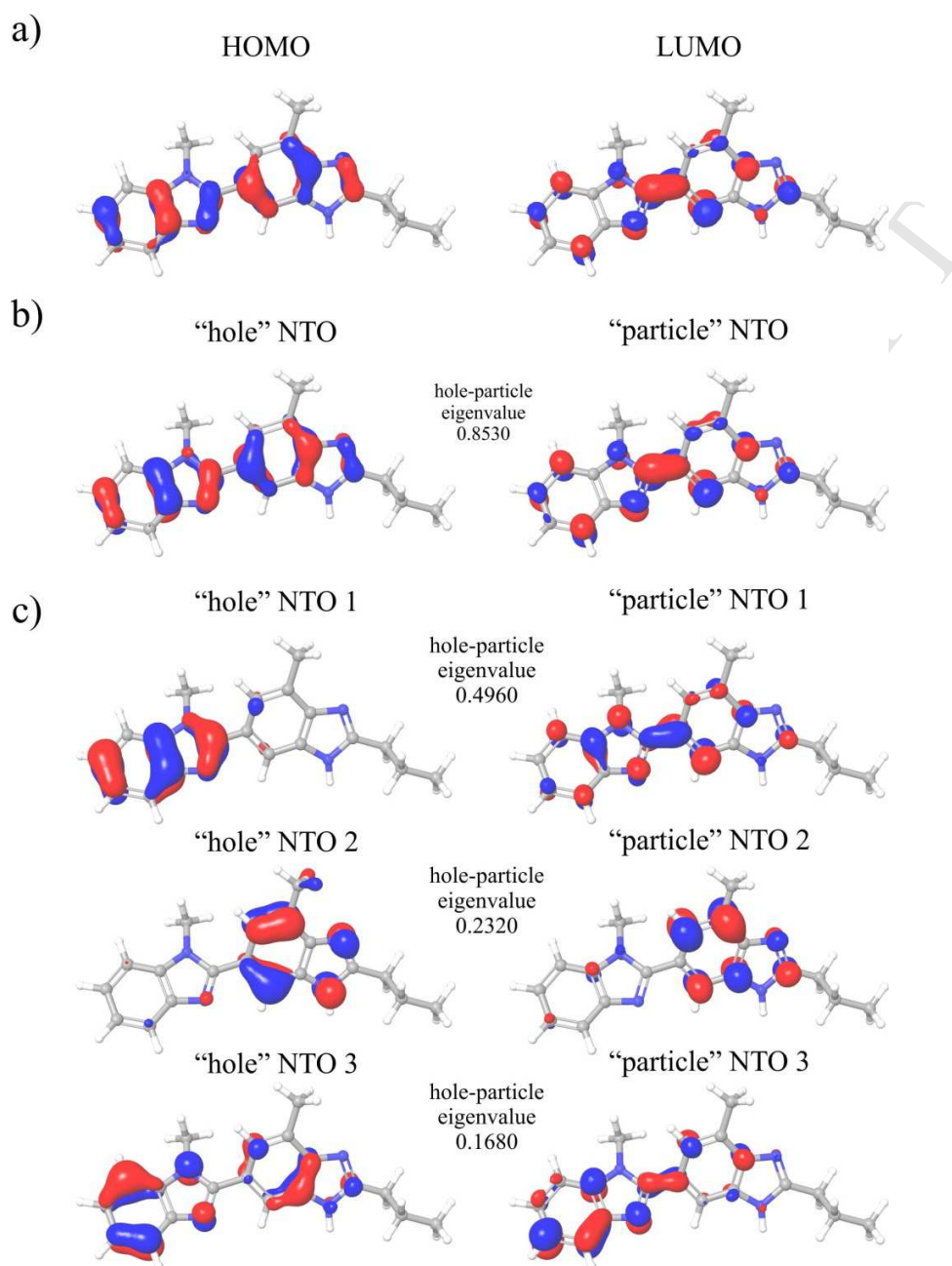


Figure 6. a) HOMO and LUMO orbitals and hole/particle NTOs of the b) first and c) sixth excitation.

Results provided in Figure 6 indicate that HOMO matches the hole NTO, while LUMO matches the particle NTO of the first excitation, meaning that frontier molecular orbitals principally

determine the absorption peak at 276 nm. The shape of HOMO and LUMO indicate that transitions are of $\pi \rightarrow \pi^*$ nature, while their distribution indicates the importance of five and six member rings when it comes the UV absorption properties. The first excitation is characterized by only one pair of NTOs (Figure 6b), while the sixth excitation is characterized by three pairs of NTOs (Figure 6c). Of three pairs of NTOs in the case of sixth excitation (and the second most important excitation according to the oscillator strength) the NTO pair 1 has the highest hole-particle eigenvalue indicating that this NTO is the most important for the absorption peak located at around 200 nm. Closer look at the NTO pair 1 indicate that the hole NTO is located almost completely at the two (left) rings without alkyl chain, while the particle NTO 1 almost completely matches the LUMO orbital. After further inspection of molecular orbitals it was concluded that the hole NTO 1 is practically the HOMO-1 orbital, so the transition from HOMO-1 to LUMO is principally responsible for absorption peak at around 200 nm.

4. Conclusions

In summary, the synthesis, spectroscopic characterization, and computational investigations of 1,7'-Dimethyl-2'-propyl-1H,3'H-[2,5']bibenzoimidazolyl was presented. The molecular structure of the compound under study was characterized with FT-IR, ^1H and ^{13}C NMR, and mass spectrometric techniques. Our computational investigations illustrate that ALIE surface recognizes three distinct molecule sites with the lowest (nitrogen atoms N5 and N23) and the highest (hydrogen atom H14) ALIE values. After MD simulations it turned out that these molecule sites are characterized with the most important interactions with water molecules. Fukui functions identified further molecule sites in the near vicinity of hydrogen atoms H28 and H34 as important reactive centers after the removal/addition of charge. DFT calculations of H-BDE show that **R4** molecule is stable towards the autoxidation mechanism with all H-BDE

values being higher than 90 kcal/mol. The most important RDF was observed in the case of hydrogen atom H14, with maximal $g(r)$ value located at the distance lower than 2 Å. TD-DFT calculations and the NTO helped in determination of the most important molecule sites when it comes to the light absorption properties. According to the shape of orbitals it can be stated that the lowest energy excitation corresponds to the $\pi \rightarrow \pi^*$ transition. Furthermore, NTO orbital pair in the case of the lowest energy excitation matches frontier molecular orbitals, thus the HOMO \rightarrow LUMO transition is principally responsible for the absorption peak at ~280 nm. According to the oscillator strengths, the second most important excitation is the sixth excitation. Analysis of the TD-DFT ordinary and NTO orbitals suggests that transition from HOMO-1 to LUMO is principally responsible for the absorption peak around 200 nm.

Acknowledgments

KSP is grateful to Dr. Mohini Gupta, Director, Manipal Centre for Natural Sciences, Manipal University for financial support (start-up grant). We thankfully acknowledge Schrödinger Inc for their support. Part of this study was conducted within the projects supported by the Ministry of Education, Science and Technological Development of Serbia, grant numbers OI 171039 and TR 34019. KSP is thankful to the Head, Department of Chemistry, MIT, Manipal University for providing FT-IR instrumental facilities.

References

1. Z. Ochal, M. Bretner, R. Wolinowska, S. Tyski, Synthesis and in vitro antibacterial activity of 5-halogenomethylsulfonyl-benzimidazole and benzotriazole derivatives, *Med. Chem.* 9 (2013) 1129-1136. <http://doi.org/10.2174/1573406411309080015>.

2. N.C. Desai, D.D. Pandya, G.M. Kotadiya, Priyanka Desai, Synthesis and characterization of novel benzimidazole bearing pyrazoline derivatives as potential antimicrobial agents, *Med. Chem. Res.* 23 (2014) 1474-1487, <http://doi.org/10.1007/s00044-013-0756>
3. K. Starcevic, M. Kralj, K. Ester, I. Sabol, M. Grace, K. Pavelic, G.K. Zambola, Synthesis, antiviral and antitumor activity of 2-substituted-5-amidino-benzimidazoles, *Bioorg. Med. Chem.* 15 (2007) 4419-4426, <http://doi.org/10.1016/j.bmc.2007.04.032>.
4. D. Yang, D. Fokas, J. Li, L. Yu, C.M. Baldino, A Versatile Method for the Synthesis of Benzimidazoles from *o*-Nitroanilines and Aldehydes in One Step via a Reductive Cyclization, *Synthesis* 1 (2005) 47-56, <http://doi.org/10.1055/s-2004-834926>.
5. (a) Y.S. Su, C.M. Sun, Microwave-Assisted Benzimidazole Cyclization by Bismuth Chloride, *Synlett.* 1 (2005) 1243-1246, <http://doi.org/10.1055/s-2005-865240>.
(b) Y.S. Su, M.J. Lin, C.M. Sun, Mercury chloride assisted cyclization toward benzimidazoles by focused microwave irradiation, *Tetrahedron Lett.* 46 (2004) 177-180, <http://doi.org/10.1016/j.tetlet.2004.10.170>.
6. L.F. Olguin, J.E. Manuel, E. Barzana, N.O. Arturo, Baker's Yeast-Mediated Regioselective Reduction of 2,4-Dinitroacylanilines: Synthesis of 2-Substituted 6-Nitrobenzimidazoles, *Synlett.* 2 (2005) 340-342, <http://doi.org/10.1055/s-2004-837203>.
7. S. Armaković, S.J. Armaković, J.P. Šetrajčić, I.J. Šetrajčić, Active components of frequently used β -blockers from the aspect of computational study. *J. Mol. Model.* 18 (2012) 4491, <http://doi.org/10.1007/s00894-012-1457-5>.
8. S.J. Armaković, S. Armaković, N.L. Finčur, F. Šibul, D. Vione, J.P. Šetrajčić, B. Abramović, Influence of electron acceptors on the kinetics of metoprolol photocatalytic degradation in

- TiO₂ suspension. A combined experimental and theoretical study, *RSC Adv.* 5 (2015) 54589-54604, <http://doi.org/10.1039/C5RA10523D>.
9. M. Blessy, R.D. Patel, P.N. Prajapati, Y. Agrawal, Development of forced degradation and stability indicating studies of drugs—A review, *J. Pharma. Analysis* 4 (2014) 159-165, <http://doi.org/10.1016/j.jpha.2013.09.003>.
 10. B. Abramović, S. Kler, D. Šojić, M. Laušević, T. Radović, D. Vione, Photocatalytic degradation of metoprolol tartrate in suspensions of two TiO₂-based photocatalysts with different surface area. Identification of intermediates and proposal of degradation pathways, *J. Hazard. Mater.* 198 (2011) 123-132, <http://doi.org/10.1016/j.jhazmat.2011.10.017>.
 11. D.D. Četojević-Simin, S.J. Armaković, D.V. Šojić, B.F. Abramović, Toxicity assessment of metoprolol and its photodegradation mixtures obtained by using different type of TiO₂ catalysts in the mammalian cell lines, *Sci. Total. Environ.* 463 (2013) 968-974, <http://doi.org/10.1016/j.scitotenv.2013.06.083>.
 12. K. Shiva Prasad, R.R. Pillai, S. Armakovic, S.J. Armakovic, Theoretical investigation on the reactivity and photophysical properties of cobalt(II) and manganese(II) complexes constructed using Schiff base ligands based on ALIE and TDDFT calculations, *Polyhedron*, 129 (2017) 141-148, <http://doi.org/10.1016/j.poly.2017.03.049>.
 13. S.W. Hovorka, C. Schöneich, Oxidative degradation of pharmaceuticals: theory, mechanisms and inhibition, *J. Pharma. Sci.* 90 (2001) 253-269. [http://doi.org/10.1002/1520-6017\(200103\)90:3](http://doi.org/10.1002/1520-6017(200103)90:3).
 14. P. Lienard, J. Gavartin, G. Boccardi, M. Meunier, Predicting drug substances autoxidation, *Pharma. Res.* 32 (2015) 300-310, <http://doi.org/10.1007/s11095-014-1463-7>.

15. G.L. De Souza, L.M. De Oliveira, R.G. Vicari, A. Brown, A DFT investigation on the structural and antioxidant properties of new isolated interglycosidic *O*-(1 → 3) linkage flavonols, *J. Mol. Model.* 22 (2016) 100-110, <http://doi.org/10.1007/s00894-016-2961-9>.
16. Z. Sroka, B. Żbikowska, J. Hładyszowski, The antiradical activity of some selected flavones and flavonols. Experimental and quantum mechanical study, *J. Mol. Model.* 21 (2015) 307-318, <http://doi.org/10.1007/s00894-015-2848-1>.
17. H. Djeradi, A. Rahmouni, Cheriti, Antioxidant activity of flavonoids: a QSAR modeling using Fukui indices descriptors, *J. Mol. Model.* 20 (2014) 2476-2485, <http://doi.org/10.1007/s00894-014-2476-1>.
18. S. Materials Science Suite 2017-1, LLC, New York, NY, 2017., Materials Science Suite, (2017).
19. A.D. Bochevarov, E. Harder, T.F. Hughes, J.R. Greenwood, D.A. Braden, D.M. Philipp, D. Rinaldo, M.D. Halls, J. Zhang, R.A. Friesner, Jaguar: A high-performance quantum chemistry software program with strengths in life and materials sciences, *Int. J. Quantum. Chem.* 113 (2013) 2110-2142, <http://doi.org/10.1002/qua.24481>.
20. D. Shivakumar, J. Williams, Y. Wu, W. Damm, J. Shelley, W. Sherman, Prediction of Absolute Solvation Free Energies using Molecular Dynamics Free Energy Perturbation and the OPLS Force Field, *J. Chem. Theory Comput.* 6 (2010) 1509-1519, <http://doi.org/10.1021/ct900587b>.
21. Z. Guo, U. Mohanty, J. Noehre, T.K. Sawyer, W. Sherman, G. Krilov, Probing the α -Helical Structural Stability of Stapled p53 Peptides: Molecular Dynamics Simulations and Analysis, *Chem. Bio. Drug Des.* 75 (2010) 348-359, <http://doi.org/10.1111/j.1747-0285.2010.00951>.

22. K.J. Bowers, E. Chow, H. Xu, R.O. Dror, M.P. Eastwood, B.A. Gregersen, J.L. Klepeis, I. Kolossvary, M.A. Moraes, F.D. Sacerdoti, Proceedings of the ACM/IEEE (2006) IEEE, 43.
23. V.B. Bregović, N. Basarić, K. Mlinarić-Majerski, Anion binding with urea and thiourea derivatives, *Coord. Chem. Rev.* 295 (2015) 80-124, <http://doi.org/10.1016/j.ccr.2015.03.011>.
24. A.D. Becke, Density-functional thermochemistry. III. The role of exact exchange, *J. Chem. Phys.* 98 (1993) 5648-5652, <http://doi.org/10.1063/1.464913>.
25. T. Yanai, D.P. Tew, N.C. Handy, A new hybrid exchange–correlation functional using the Coulomb-attenuating method (CAM-B3LYP), *Chem. Phys. Lett.* 393 (2004) 51-57, <http://doi.org/10.1016/j.cplett.2004.06.011>.
26. E. Harder, W. Damm, J. Maple, C. Wu, M. Reboul, J.Y. Xiang, L. Wang, D. Lupyan, M.K. Dahlgren, J.L. Knight, OPLS3: A Force Field Providing Broad Coverage of Drug-like Small Molecules and Proteins, *J. Chem. Theory Comput.* 12 (2015) 281-296, <http://doi.org/10.1021/acs.jctc.5b00864>.
27. W.L. Jorgensen, D.S. Maxwell, J. Tirado Rives, Development and Testing of the OPLS All-Atom Force Field on Conformational Energetics and Properties of Organic Liquids, *J. Am. Chem. Soc.* 118 (1996) 11225-11236, <http://doi.org/10.1021/ja9621760>.
28. W.L. Jorgensen, J. Tirado-Rives, The OPLS Force Field for Proteins. Energy Minimizations for Crystals of Cyclic Peptides and Crambin, *J. Am. Chem. Soc.* 110 (1988) 1657-1666, <http://doi.org/10.106/ja00214a001>.
29. H.J. Berendsen, J.P. Postma, W.F. Van Gunsteren, J. Hermans, Interaction Models for Water in Relation to Protein Hydration, Springer (1981) 331-342, http://doi.org/10.1007/978-94-015-7658-1_21.

30. A. Otero-de-la-Roza, E.R. Johnson, J. Contreras-García, Revealing non-covalent interactions in solids: NCI plots revisited, *Phy. Chem. Chem. Phys.* 14 (2012) 12165-12172, <http://doi.org/10.1039/C2CP41395G>.
31. E.R. Johnson, S. Keinan, P. Mori-Sanchez, J. Contreras-Garcia, A.J. Cohen, W. Yang, Revealing Noncovalent Interactions, *J. Am. Chem. Soc.* 132 (2010) 6498-6506, <http://doi.org/10.1021/ja100936w>.
32. Schrödinger Release 2017-1: Maestro, Schrödinger, LLC, New York, NY, (2017) 2017.
33. I. Nagao, T. Ishizaka, H. Kawanami, Rapid production of benzazole derivatives by a high-pressure and high-temperature water microflow chemical process, *Green Chem.* 18 (2016) 3494-3498, <http://doi.org/10.1039/C6GC01195K>.
34. J.S. Murray, J.M. Seminario, P. Politzer, P. Sjoberg, Average local ionization energies computed on the surfaces of some strained molecules, *Int. J. Quantum Chem.* 38 (1990) 645-653, <http://doi.org/10.1002/qua.560382462>.
35. P. Politzer, F. Abu-Awwad, J.S. Murray, Comparison of density functional and Hartree-Fock average local ionization energies on molecular surfaces, *Int. J. Quantum Chem.* 69 (1998) 607-613, [http://doi.org/10.1002/\(SICI\)1097-461](http://doi.org/10.1002/(SICI)1097-461).
36. F.A. Bulat, A. Toro-Labbé, T. Brinck, J.S. Murray, P. Politzer, Quantitative analysis of molecular surfaces: areas, volumes, electrostatic potentials and average local ionization energies, *J. Mol. Model.* 16 (2010) 1679-1691, <http://doi.org/10.1007/s00894-010-0692>.
37. P. Politzer, J.S. Murray, F.A. Bulat, Average local ionization energy: A review, *J. Mol. Model.* 16 (2010) 1731-1742, <http://doi.org/10.1007/s00894-010-0709-5>.

38. M.D. Esrafil, Nitrogen-doped (6, 0) carbon nanotubes: a comparative DFT study based on surface reactivity descriptors. *Comput. Theo. Chem.* 1015 (2013) 1-7, <http://doi.org/10.1016/j.comptc.2013.04.003>.
39. J.V. Burda, Z. Futera, and Z. Chval, Exploration of various electronic properties along the reaction coordinate for hydration of Pt (II) and Ru (II) complexes; the CCSD, MPx, and DFT computational study. *J. Mol. Model.* 19 (2013) 5245-5255, <http://doi.org/10.1007/s00894-013-1994-6>.
40. J.I. Martínez-Araya, Revisiting caffeine's capabilities as a complexation agent to silver cation in mining processes by means of the dual descriptor—a conceptual DFT approach. *J. Mol. Model.* 18 (2012) 4299-4307, <http://doi.org/10.1007/s00894-012-1405-4>.
41. T. Zábajňáková, R. Cajzl, J. Kljun, Z. Chval, I. Turel, and J.V. Burda, Interactions of the “piano-stool”[ruthenium(II)(η^6 -arene)(quinolone)Cl]⁺ complexes with water; DFT computational study. *J. Comput. Chem.* 37 (2016), 1766-1780, <http://doi.org/10.1002/jcc.24373>.
42. A. Michalak, F. De Proft, P. Geerlings, R. Nalewajski, Fukui Functions from the Relaxed Kohn–Sham Orbitals, *J. Phy. Chem. A.* 103 (1999) 762-771, <http://doi.org/10.1021/jp982761i>.
43. X. Ren, Y. Sun, X. Fu, L. Zhu, Z. Cui, DFT comparison of the OH-initiated degradation mechanisms for five chlorophenoxy herbicides, *J. Mol. Model.* 19 (2013) 2249-2263, <http://doi.org/10.1007/s00894-013-1760-9>.
44. L. Ai, J.Y. Liu, Mechanism of OH-initiated atmospheric oxidation of E/Z-CF₃CF = CFCF₃: a quantum mechanical study, *J. Mol. Model.* 20 (2014) 2179-2188, <http://doi.org/10.1007/s00894-014-2179-7>.

45. W. Sang-aroon, V. Amornkitbamrung, V. Ruangpornvisuti, A density functional theory study on peptide bond cleavage at aspartic residues: direct vs cyclic intermediate hydrolysis, *J. Mol. Model.* 19 (2013) 5501-5513, <http://doi.org/10.1007/s00894-013-2054>.
46. J. Kieffer, É. Brémond, P. Lienard, G. Boccardi, In silico assessment of drug substances chemical stability, *J. Mol. Struc.* 954 (2010) 75-79, <http://doi.org/10.1016/j.theochem.2010.03.032>.
47. K.A. Connors, G.L. Amidon, V.J. Stella, *Chemical stability of pharmaceuticals. A handbook for pharmacists*. 2nd ed. Epinephrine: John Wiley & Sons (1986) pp 438–447.
48. D. Johnson, L. Gu, *Encyclopedia of pharmaceutical technology*. 1st ed. Marcel Dekker; New York (1988) 415-449.
49. J.S. Wright, H. Shadnia, L.L. Chepelev, Stability of carbon-centered radicals: effect of functional groups on the energetics of addition of molecular oxygen, *J. Comput. Chem.* 30 (2009) 1016-1026, <http://doi.org/10.1002/jcc.21124>.
50. G. Gryn'ova, J.L. Hodgson, M.L. Coote, Revising the mechanism of polymer autooxidation, *Org. Biomole. Chem.* 9 (2011) 480-490, <http://doi.org/10.1039/c0ob00596>.
51. T. Andersson, A. Broo, E. Evertsson, Prediction of drug candidates' sensitivity toward autoxidation: computational estimation of C-H dissociation energies of carbon-centered radicals, *J. Pharma. Sci.* 103 (2014) 1949-1955, <http://doi.org/10.1002/jps.23986>.
52. R.V. Vaz, J.R. Gomes, and C.M. Silva, *Molecular dynamics simulation of diffusion coefficients and structural properties of ketones in supercritical CO₂ at infinite dilution*. *J. Supercrit. Fluids* 107 (2016) 630-638, <http://doi.org/10.1016/j.supflu.2015.07.025>.

53. N. Michaud-Agrawal, E.J. Denning, T.B. Woolf, and O. Beckstein, MDAnalysis: a toolkit for the analysis of molecular dynamics simulations. *J Comput. Chem.* 32 (2011) 2319-2327, <http://doi.org/10.1002/jcc.21787>.
54. J. Palmer, A. Llobet, S.-H. Yeon, J. Fischer, Y. Shi, Y. Gogotsi, and K. Gubbins, Modeling the structural evolution of carbide-derived carbons using quenched molecular dynamics. *Carbon*, 48 (2010) 1116-1123, <http://doi.org/10.1016/j.carbon.2009.11.033>.
55. E. Mosconi, C. Quarti, T. Ivanovska, G. Ruani, and F. De Angelis, Structural and electronic properties of organo-halide lead perovskites: a combined IR-spectroscopy and ab initio molecular dynamics investigation. *Phys. Chem. Chem. Phys.* 16 (2014) 16137-16144, <http://doi.org/10.1039/C4CP00569D>.
56. S. Feng and G.A. Voth, Molecular dynamics simulations of imidazolium-based ionic liquid/water mixtures: Alkyl side chain length and anion effects. *Fluid Phase Equilib.* 294 (2010) 148-156, <http://doi.org/10.1016/j.fluid.2010.02.034>.
57. M. Vraneš, S. Armaković, A. Tot, S. Papović, N. Zec, S. Armaković, N. Banić, B. Abramović, and S. Gadžurić, Structuring of water in the new generation ionic liquid—Comparative experimental and theoretical study. *J. Chem. Thermodyn.* 93 (2016) 164-171, <http://doi.org/10.1016/j.jct.2015.10.001>.
58. M. Vraneš, A. Tot, S. Armaković, S. Armaković, and S. Gadžurić, Structure making properties of 1-(2-hydroxyethyl)-3-methylimidazolium chloride ionic liquid. *J. Chem. Thermodyn.* 95 (2016) 174-179, <http://doi.org/10.1016/j.jct.2015.12.012>.
59. A. Tot, S. Armaković, S. Armaković, S. Gadžurić, and M. Vraneš, Kosmotropism of newly synthesized 1-butyl-3-methylimidazolium taurate ionic liquid: Experimental and

- computational study. *J. Chem. Thermodyn.* 94 (2016) 85-95, <http://doi.org/10.1016/j.jct.2015.10.026>.
60. S. Gadžurić, A. Tot, S. Armačić, S. Armačić, J. Panić, B. Jović, and M. Vraneš, Uncommon structure making/breaking behaviour of cholinium taurate in water. *J. Chem. Thermodyn.* 107 (2017) 58-64, <http://doi.org/10.1016/j.jct.2016.12.025>.
61. M. Vraneš, I. Borišev, A. Tot, S. Armačić, S. Armačić, D. Jović, S. Gadžurić, and A. Djordjevic, Self-assembling, reactivity and molecular dynamics of fullereneol nanoparticles. *Phys. Chem. Chem. Phys.* 19 (2017) 135-144, <http://doi.org/10.1039/C6CP06847B>.
62. R.L. Martin, Natural transition orbitals, *J. Chem. Phys.* 118 (2003) 4775-4777, <http://doi.org/10.1063/1.1558471>.

Highlights

- ❖ 1,7'-Dimethyl-2'-propyl-1H,3'H-[2,5']bibenzo-imidazolyl was synthesized by novel approach.
- ❖ Synthesized compound was characterized by FT-IR, NMR and MS.
- ❖ The DFT and TD-DFT calculations, and molecular dynamics have been assessed.
- ❖ Bond dissociation energies were calculated to determine autoxidation mechanism.

Graphical Abstract (synopsis)

1,7'-Dimethyl-2'-propyl-1H,3'H-[2,5']bibenzoimidazolyl was synthesized by acylation/dehydration condensation sequence of 3-methylbenzene-1,2-diamine with m-tolyl derivative in the presence of dibutyltin dilaurate (DBTDL) as catalyst. The computational investigations of global and local reactive properties based on the density functional theory (DFT) and time dependent density functional theory (TD-DFT) calculations, and molecular dynamics.